1′-(Diphenylphosphino)ferrocenecarboxylic Acid and Its *P*-Oxide and Methyl Ester: Synthesis, Characterization, Crystal Structure, and Electrochemistry

Jaroslav Podlaha,* Petr Štěpnička, Jiří Ludvík,† and Ivana Císařová

Department of Inorganic Chemistry, Charles University, 12840 Prague, Czech Republic

Received July 10, 1995[⊗]

The ferrocene derivative (η^5-$C_5H_4PPh_2$)Fe(η^5-C_5H_4COOH) (**3**), a potential hybrid phosphine ligand with heteroannular soft and hard donor groups, was synthesized in 71% yield from 1-phenyl-1-phospha[1]ferrocenophane by ring opening with phenyllithium, followed by reaction with carbon dioxide and acidification. Oxidation of **3** with hydrogen peroxide and its esterification with diazomethane provided the derivatives, phosphine oxide **4** and methyl ester **5**, respectively. The new compounds were characterized by IR, UV/vis, MS, and NMR spectroscopy, the degenerate ^{1}H NMR spectra being assigned with the aid of selective ^{1}H-{^{1}H} decoupling, ^{1}H,^{1}H-COSY, ^{13}C HMQC, and ^nJ(P,C) from APT. The solid-state structures of **3**−**5** were determined by single-crystal X-ray diffraction. Voltammetric measurements of **3**−**5** and related monosubstituted derivatives in acetonitrile revealed that the phosphines are first oxidized to the corresponding ferrocenium derivatives which are then the subject of the intramolecular electron transfer from the phosphine group to iron, the resulting species being immediately stabilized by further electrochemical and/or chemical oxidation to give phosphine oxides. The second independent electrochemical process is the reversible oxidation of these ferrocene/phosphine oxides to ferrocenium/phosphine oxides. There are further electrochemical processes associated with the irreversible oxidation of the carboxyl group.

Introduction

The coordination chemistry of phosphinoferrocenes has been the subject of substantial investigation over the past 2 decades. In particular, the heteroannular bis(phosphines) such as 1,1′-bis(diphenylphosphino)ferrocene attract much interest because their complexes find synthetic applications in transition-metal-catalyzed processes. Less attention has been paid to related phosphinoferrocenes which posses a hard-donor functional group instead of the second phosphine center. These ligands belong to the class of "hybrid" phosphines which are capable of coordinating by a number of ways depending mainly on the metal hardness. Representative examples of such hard donors in phosphinoferrocenes include 2,2′-bipyridyl,[1] Schiff bases,[2] and macrocycles[3,4] as the hard donor functionality. In our laboratory, tertiary phosphines with carboxyl group(s) as the second donor have been studied.[5] They are formally analogous to the familiar amino polycarboxylates and constitute two series, $R_{3-n}P(CH_2COOH)_n$ (n = 1−3; R = Ph, Me, Et, *i*-Pr) and [−$CH_2P(CH_2COOH)_n$-Ph_{2-n}]$_2$ (n = 1, 2). These substituted phosphines form secondary metal−carboxylate bonds which may be cleaved reversibly on changing pH to open a coordination site on the metal, necessary for the induction of catalytic activity. Moreover, the ligands and complexes with n > 1 are often water-soluble and may be used as selective and effective extractants of platinum metals from organic into aqueous phase.[6] In this paper, we report the synthesis and properties of a new ligand bearing the given combination of the donor groups on the ferrocene backbone.

Scheme 1

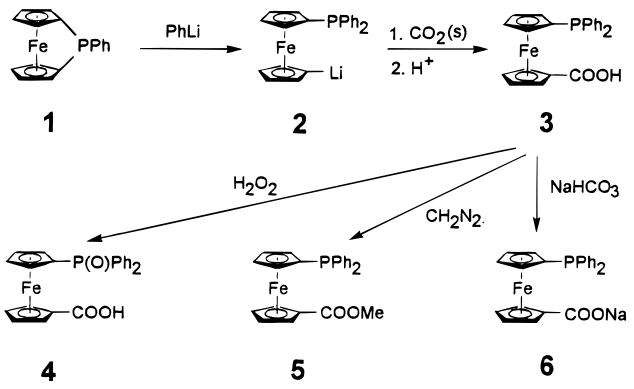

† Current address: J. Heyrovský Institute of Physical Chemistry, Academy of Sciences of the Czech Republic, 18223 Prague, Czech Republic.

⊗ Abstract published in *Advance ACS Abstracts,* December 1, 1995.

(1) Butler, I. R.; Kalaji, M.; Nehrlich, L.; Hursthouse, M.; Karaulov, A. I.; Abdul Malik, K. M. *J. Chem. Soc., Chem. Commun.* **1995**, 459.

(2) Houlton, A.; Jasim, N.; Roberts, R. M. G.; Silver, J.; Cunningham, D.; McArdle, P.; Higgins, T. *J. Chem. Soc., Dalton Trans.* **1992**, 2235.

(3) Beer, P. D.; Nation, J. E.; McWhinnie, S. L. W.; Harman, M. E.; Hursthouse, M. B.; Ogden, M. I.; White, A. H. *J. Chem. Soc., Dalton Trans.* **1991**, 2485.

(4) Grossel, M. C.; Goldspink, M. R.; Knychala, J. P.; Cheetham, A. K.; Hriljac, J. A. *J. Organomet. Chem.* **1988**, *352*, C13.

(5) (a) Podlahová, J.; Kratochvíl, B.; Podlaha, J.; Hašek, J. *J. Chem. Soc., Dalton Trans.* **1985**, 2393 and references therein. (b) Podlaha, J.; Jegorov, A.; Buděšínský, M.; Hanuš, V. *Phosphorus Sulfur* **1988**, *37*, 87 and references therein. (c) Podlahová, J.; Hartl, F.; Podlaha, J.; Knoch, F. Polyhedron **1987**, *6*, 1987 and references therein.

(6) Jegorov, A.; Podlaha, J. *Catal. Lett.* **1991**, *8*, 9.

0276-7333/96/2315-0543$12.00/0

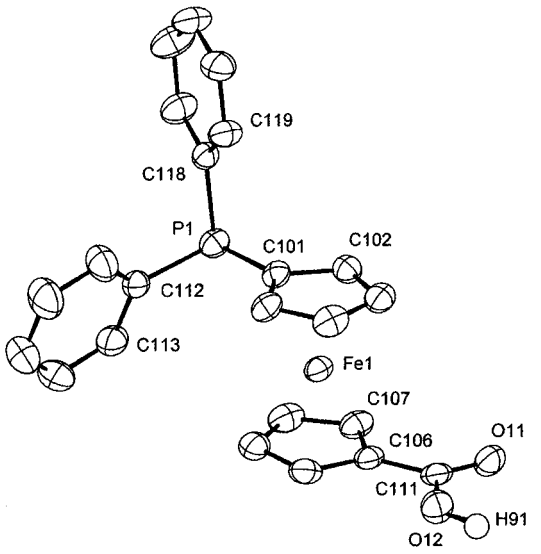

Figure 1. ORTEP plot of the molecule of **3** at 40% probability level. For clarity, calculated hydrogen atoms are omitted and only pivot and adjacent carbon atoms of the rings are labeled.

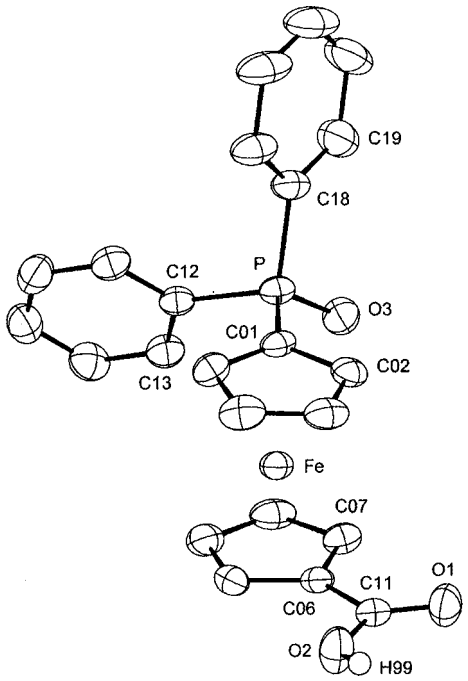

Figure 2. ORTEP plot of the molecule of **4** at 40% probability level. For clarity, calculated hydrogen atoms are omitted and only pivot and adjacent carbon atoms of the rings are labeled.

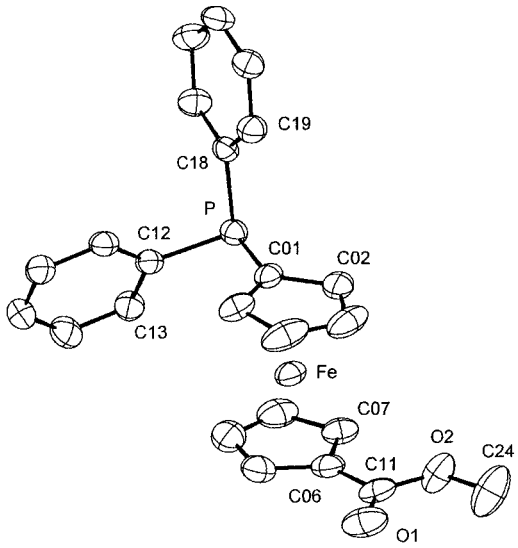

Figure 3. ORTEP plot of the molecule of **5** at 40% probability level. For clarity, calculated hydrogen atoms are omitted and only pivot and adjacent carbon atoms of the rings are labeled.

Results and Discussion

Synthesis. According to Scheme 1, ring opening[7] of 1-phenyl-1-phospha- [1]ferrocenophane (**1**)[8] with phenyllithium gave the lithiated derivative **2** which was reacted *in situ* with excess solid carbon dioxide; the subsequent acidification provided 1′-(diphenylphosphino)ferrocenecarboxylic acid (**3**) in 71% yield. The standard oxidation of **3** with hydrogen peroxide in acetone produced phosphine oxide **4** in 43% yield, and the reaction of **3** with diazomethane in Et_2O led to methyl ester **5** in 71% yield (yields not optimized). Sodium salt **6** is formed by neutralization of **3** with sodium hydrogen carbonate in ethanol or with sodium hydroxide in aqueous ethanol, but it could not be isolated in pure form (IR of a crude hygroscopic material in Nujol: 1345, 1540 cm^{-1}, COO^-). Attempts to isolate the K or Rb salt were also unsuccessful, even in the presence of alkali-metal complexing agents such as linear and cyclic polyethers. Compounds **3**−**6** are soluble in polar organic solvents (**6** also in water) to give orange solutions (yellow for **6**) which, for phosphines **3**, **5**, and **6**, are oxidized slowly in air. Solid samples of **3**−**5** are air-stable; **3** and **5** are orange in color, and **4** is rusty red.

Crystal Structures. The solid-state structures of compounds **3**−**5** were determined by single-crystal X-ray diffraction. Since the position of the substituents on the cyclopentadienyl rings is neither exactly *anti*-staggered nor exactly *syn*-eclipsed, the molecules display planar chirality in the crystal with both enantiomers present in the racemic crystal. Further, the asymmetric unit of **3** contains two symmetrically independent but chemically almost identical molecules labeled 1 and 2. The arrangement of molecules *(R)*-**3** (molecule 1), *(R)*-**4**, and *(R)*-**5** (Figures 1−3) is very similar. It consists of nearly parallel cyclopentadienyl rings (the tilt angles are less than 3°; see the Supporting Information for details) bearing the heteroannular substituents in *anti* arrangement. All intramolecular bond distances and angles are unexceptional; selected values are summarized in Table 1. There are significant conformational differences between the three molecules. Major changes are encountered, of course, at the places where the molecules differ chemically. As manifested by the dihedral angles of the mean phenyl and cyclopentadienyl planes (Supporting Information), the distortion of the approximately tetrahedral environment of phosphorus reflects different steric requirement of oxygen in **4** and of the electron pair in **3** and **5**. At the opposite end of the molecules, the carboxyl groups are nearly coplanar with the parent cyclopentadienyl rings but the carboxylate group in ester **5** is turned over by 180° with respect to carboxylic acids **3** and **4**. There are further less obvious but

(7) (a) Seyferth, D.; Withers, H. P., Jr. *J. Organomet. Chem.* **1980**, *185*, C1. (b) Seyferth, D.; Withers, H. P. *Organometallics* **1982**, *1*, 1275.
(8) Osborne, A. G.; Whiteley, R. H.; Meads, R. E. *J. Organomet. Chem.* **1980**, *193*, 345.

Table 1. Selected Bond Lengths (Å) and Angles (deg) for 3−5

3							
molecule 1		molecule 2		4		5	
(a) Bond Lengths							
Fe−C in Cp (mean) 2.048(5)					2.04(1)		2.037(7)
C−C in Cp (mean) 1.42(1)					1.41(1)		1.41(1)
C−C in Ph (mean) 1.38(1)					1.38(1)		1.380(9)
				P−O(3)	1.487(2)		
P(1)−C(101)	1.820(5)	P(2)−C(201)	1.814(5)	P−C(01)	1.787(3)	P−C(01)	1.808(2)
P(1)−C(112)	1.842(5)	P(2)−C(212)	1.833(5)	P−C(12)	1.795(3)	P−C(12)	1.835(2)
P(1)−C(118)	1.837(4)	P(2)−C(218)	1.830(4)	P−C(18)	1.808(3)	P−C(18)	1.839(2)
C(111)−O(11)	1.228(5)	C(211)−O(21)	1.228(5)	O(1)−C(11)	1.200(4)	O(1)−C(11)	1.204(3)
C(111)−O(12)	1.314(5)	C(211)−O(22)	1.315(5)	O(2)−C(11)	1.318(4)	O(2)−C(11)	1.333(3)
						O(2)−C(24)	1.439(4)
(b) Bond Angles							
C−C−C in Cp (mean) 108.0(6)					108.0(5)		108.0(7)
C−C−C in Ph (mean) 120(1)					120.0(7)		120(1)
O(11)−C(111)−O(12)	123.2(5)	O(21)−C(211)−O(22)	123.7(5)	O(1)−C(11)−O(2)	124.3(3)	O(1)−C(11)−O(2)	123.5(3)
						C(11)−O(2)−C(24)	117.0(3)
O(11)−C(111)−C(106)	122.0(5)	O(21)−C(211)−C(206)	122.2(4)	O(1)−C(11)−C(06)	122.6(3)	O(1)−C(11)−C(06)	125.0(3)
O(12)−C(111)−C(106)	114.8(5)	O(22)−C(211)−C(206)	114.1(5)	O(2)−C(11)−C(06)	113.1(3)	O(2)−C(11)−C(06)	111.4(2)
C(107)−C(106)−C(111)	124.2(4)	O(207)−C(206)−C(211)	128.1(4)	C(07)−C(06)−C(11)	123.6(3)	C(07)−C(06)−C(11)	127.4(2)
C(110)−C(106)−C(111)	127.7(4)	C(210)−C(206)−C(211)	124.1(4)	C(10)−C(06)−C(11)	128.8(3)	C(10)−C(06)−C(11)	124.6(3)
				O(3)−P−C(01)	113.2(1)		
				O(3)−P−C(12)	113.7(1)		
				O(3)−P−C(18)	109.8(2)		
C(101)−P(1)−C(112)	100.9(2)	C(201)−P(2)−C(212)	101.3(2)	C(01)−P−C(12)	106.4(1)	C(01)−P−C(12)	101.5(1)
C(101)−P(1)−C(118)	100.2(2)	C(201)−P(2)−C(218)	100.2(2)	C(01)−P−C(18)	106.6(1)	C(01)−P−C(18)	101.0(1)
C(112)−P(1)−C(118)	102.3(2)	C(212)−P(2)−C(218)	102.4(2)	C(12)−P−C(18)	106.8(1)	C(12)−P−C(18)	101.5(1)
C(102)−C(101)−P(1)	123.6(3)	C(202)−C(201)−P(2)	123.8(3)	C(02)−C(01)−P	124.0(2)	C(02)−C(01)−P	123.9(2)
C(105)−C(101)−P(1)	129.7(3)	C(205)−C(201)−P(2)	129.4(3)	C(05)−C(01)−P	128.7(2)	C(05)−C(01)−P	129.5(2)
C(113)−C(112)−P(1)	117.3(4)	C(213)−C(212)−P(2)	118.4(4)	C(13)−C(12)−P	118.4(2)	C(13)−C(12)−P	117.8(2)
C(117)−C(112)−P(1)	124.5(4)	C(217)−C(212)−P(2)	124.6(4)	C(17)−C(12)−P	123.0(2)	C(17)−C(12)−P	124.2(2)
C(119)−C(118)−P(1)	124.0(3)	C(219)−C(218)−P(2)	124.0(3)	C(19)−C(18)−P	118.2(3)	C(19)−C(18)−P	124.3(2)
C(123)−C(118)−P(1)	118.0(4)	C(223)−C(218)−P(2)	118.6(4)	C(23)−C(18)−P	122.8(3)	C(23)−C(18)−P	117.4(2)

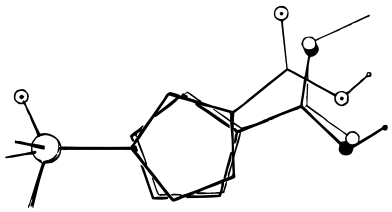

Figure 4. Superposition of molecules **3** (thick lines) and **4** and **5** (thin lines) viewed from the side of the P-substituted Cp ring.

significant differences between the three molecules in the mutual position of the phosphine and carboxyl substituents. Figure 4 depicts the superposition of the appropriate fragments, oriented perpendicularly to the cyclopentadienyl rings from the side of the P-substituted ring (i.e., according to the chirality preference). It appears that the *anti*-conformation of the substituted cyclopentadienyls is exactly halfway between staggered and eclipsed in phosphines **3** and **5** but, in contrast, perfectly eclipsed in phosphine oxide **4**. This is best demonstrated by the torsion angle τ defined by the P-bearing carbon C(01), the cyclopentadienyl centroids, and the carboxyl-bearing carbon C(06). The value of τ is 162.0(4)° for **3** and 161.8(4)° for **5** but 141.9(3)° for **4**, the theoretical τ's being 180° for the fully staggered and 144° for the fully eclipsed *anti*-conformation. A search of the Cambridge Structural Database for 1,1′-disubstituted ferrocenes (free of intramolecular steric constraints such as transannular links) revealed that the *syn*- and *anti*-conformations of the 1,1′-substituents are preferred but other arrangements are also quite common (see the Supporting Information for the data). From the closely related compounds, the carboxyl groups are exactly *syn*-eclipsed, possibly as the result of hydrogen bonding, while the bulky PPh_2 groups of 1,1′-bis(diphenylphosphino)ferrocene are exactly *anti*-staggered. Clearly, the particular conformation of the cyclopentadienyls rings is dictated by subtle factors of which the crystal packing is undoubtedly imperative. The interaction of molecules **3**−**5** and **5** in the crystalline state differs, in fact, considerably. In **3**, each of the two independent molecules is linked to its centrosymmetric partner through a 2-fold hydrogen bond, resulting in dimers which are then packed at the normal van der Waals distances. The molecules of phosphine oxide **4** are associated by intermolecular hydrogen bonding [O···O, 2.588(3) Å] between the carboxylic hydroxyl and the P═O oxygen which links the molecules into zigzag chains running along the crystallographic *b* direction. Finally, the structure of ester **5** is molecular with no contacts shorter than the sum of the van der Waals radii. These different types of crystal packing are nicely reflected on the mass spectra and mp's (see Experimental Section).

NMR Spectra. The ^1H and ^{31}P NMR spectra of compounds **3**−**5** and the ^{13}C spectra of **3** are summarized in Tables 2 and 3; atom labels are defined in Chart 1 (hydrogens are labeled according to their bonding carbons). In phosphine carboxylic acid **3**, the cyclopentadienyl protons of the P-substituted ring behave as an AA′BB′X spin system (X = P) and those of the COOH-substituted ring as an AA′BB′ system. The signal of the carboxyl proton was not observed. The spin−spin interactions deduced from the degenerate ^1H spectra by selective $^1H\{^1H\}$ decoupling were confirmed by $^1H \leftrightarrow {}^1H$ correlations (^1H,^1H-COSY: 4.17 ↔ 4.45; 4.34 ↔ 4.76), $^{13}C \leftrightarrow {}^1H$ correlations (^{13}C HMQC; see Table 3), and by the ^nJ(P,C) interaction constants (from APT).

Table 2. ^{1}H and ^{31}P NMR Data for 3−5

compd	^{1}H chem shift[a] for protons (multiplicity,[b] rel intensity) 2, 5	3, 4	2′, 5′	3′, 4′	others	^{31}P chem shift[c]
3	4.76 (t, 2H)	4.34 (t, 2H)	4.17 (q, 2H)	4.45 (t, 2H)	phenyl, 7.30−7.37 (m, 10H)	−17.6
4	5.06 (t, 2H)	4.31 (t, 2H)	4.60 (q, 2H)	4.37 (q, 2H)	phenyl, 7.43−7.64 (m, 6H), 7.67−7.79 (m, 4H)	+32.9
5	4.71 (t, 2H)	4.17 (t, 2H)	4.13 (q, 2H)	4.39 (t, 2H)	phenyl, 7.29−7.42 (m, 10H); methyl, 3.17 (s, 3H)	−17.4

[a] Measured at room temperature in C[^{2}H]Cl$_3$ with TMS as internal standards. [b] s = singlet, t = triplet, and q = quadruplet. [c] Measured at room temperature in C[^{2}H]Cl$_3$ with 85% aqueous H_3PO_4 as external standards.

Table 3. ^{13}C NMR Shifts and Heteronuclear Correlations for 3

signal	δ(^{13}C)[a] (mult[b])	^{1}H correlation (from ^{13}C HMQC)
	Cp	
1	70.4 (s)	
2, 5	71.4 (s)	4.76
3, 4	73.4 (d, J = 1.5 Hz)	4.34
1′	78.4 (d, J = 9.2 Hz)	
2′, 5′	74.4 (d, J = 14.5 Hz)	4.17
3′, 4′	73.3 (d, J = 3.0 Hz)	4.45
	Ph	
i	138.4 (d, J = 9.9 Hz)	
o	133.5 (d, J = 19.8 Hz)	
m	128.3 (d, J = 6.9 Hz)	7.30−7.37
p	128.7 (s)	
	C=O	
	177.2 (s)	

[a] Measured at room temperature in C[^{2}H]Cl$_3$, indirect internal reference C[^{2}H]Cl$_3$ (δ 77.0). [b] s = singlet and d = doublet.

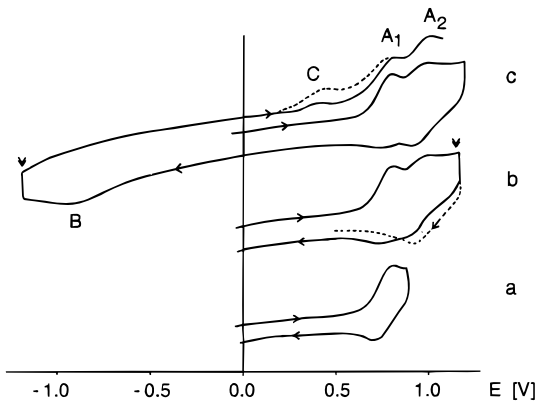

Figure 5. Cyclic voltammograms of **3**. Curves a−c correspond to different switch potentials, and dotted lines, to measurement after electrolysis at potentials labeled by double arrows.

Chart 1

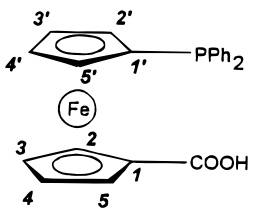

Further discussion of NMR spectra is presented as Supporting Information.

Electrochemistry. Compounds **3**−**5** and related monosubstitued ferrocenes were studied by voltammetry with a rotating disk platinum electrode (RDE) and by cyclic voltammetry (CV) with a stationary platinum electrode. There are several redox processes involved (Figure 5; Table 4) which, in analogy to the known electrochemical behavior of monosubstituted ferrocenes[9] and 1,1′-(diphenylphosphino)ferrocene,[10] may be classified as belonging to three groups labeled A−C.

Process A—the main anodic reaction—is in all cases the reversible one-electron oxidation of the ferrocene skeleton yielding the corresponding ferrocenium. It can be subdivided into processes A_1 and A_2 (Figures 5 and 6). In contrast to the oxidation of phosphines (compounds FcPPh$_2$, **3**, and **5**) where both processes A_1 and A_2 are involved, only the reversible process A_2 takes place for phosphine oxides (FcP(O)Ph$_2$ and **4**).

From the comparison of the redox behavior of analogous P^{III} and P^V derivatives (FcPPh$_2$, FcP(O)Ph$_2$ and **3**, **4**, respectively), it is evident that process A_2 in the case of P^{III} compounds corresponds to the single ferrocene−ferrocenium redox process for phosphine oxides. It follows that the phosphine oxides are generated in situ from P^{III} derivatives during the first anodic A_1 reaction.

If the switching potential in CV of phosphines lies close to the anodic peak of A_1 (but before A_2), a small cathodic peak corresponding to A_1 redox couple appears and gains in intensity with increasing sweep rate. If the switching potential is more positive by 200−250 mV (*i.e.*, after A_2), the reversible couple of anodic/cathodic peaks belonging to A_2 dominates and, simultaneously, the cathodic peak of A_1 becomes smaller. Short electrolysis at the switching potential during CV causes this peak to disappear totally. These observations are indicative of a subsequent chemical oxidation which follows the first electron transfer.

As summarized in Scheme 2, the first process for phosphine-substituted ferrocenes is the oxidation of Fe^{II} to Fe^{III} (A_1). The resulting ferrocenium is the subject of the intramolecular electron transfer from the phosphine group to iron (*via* cyclopentadienyl), the resulting species being immediately stabilized by further one-electron oxidation (electrochemical and/or chemical by traces of oxygen or water[11]) to give phosphine oxide. The phosphine oxides originated in this way manifest themselves as the reversible redox system A_2 (Figure 6). The proposed mechanism is in agreement with the high susceptibility of ferrocene derivatives to electrophilic substitution.[12]

The redox potentials of RDE voltammetric waves for process *A* are shifted in the positive direction against the unsubstituted ferrocene by +190, +170, and +50 mV for FcCOOH, FcP(O)Ph$_2$, and FcPPh$_2$, respectively. This remarkable positive shift is undoubtedly caused

(9) (a) Little, W. F.; Reilley, C. N.; Johnson, J. D.; Sanders, A. P. *J. Am. Chem. Soc.* **1964**, *86*, 1382. (b) Scholl, H.; Sochaj, K. *Electrochim. Acta* **1991**, *36*, 689.

(10) Pilloni, G.; Longato, B.; Corain, B. *J. Organomet. Chem.* **1991**, *420*, 57.

(11) Acetonitrile is known to be notoriously difficult to dry below 10 ppm level (see, e.g.: Burfield, D. R.; Lee, K. H.; Smithers, R. H. *J. Org. Chem.* **1977**, *42*, 3060); this amount corresponds, however, to the same order of molar concentration as that of the compounds studied.

(12) Rosenblum, M.; Santer, J. O.; Glenn, H. W. *J. Am. Chem. Soc.* **1963**, *85*, 1450.

Table 4. Electrochemical Behavior of 3−5 and Related Derivatives[a]

	cyclic voltammetry						voltammetry on RDE		
	A_1		A_2		B	C	A_1	A_2	B
compd	E_{pa}	E_{pc}	E_{pa}	E_{pc}	E_{pc}	E_{pa}	$E_{1/2}$	$E_{1/2}$	$E_{1/2}$
FcH	0.47	0.39					0.44		
FcCOOH	0.65	0.60			−0.97	0.33	0.63		−0.81
$FcP(O)Ph_2$			0.64	0.59				0.61	
$FcPPh_2$	0.52	0.47	0.65	0.60			0.49	0.63	
3	0.78	0.69	0.98	0.90	−0.99	0.39	0.75		−0.80
4			0.98	0.90	−0.75	0.54		0.93	−0.66
5	0.78	0.68	0.88	0.80			0.75		

[a] All values in *V*; see text for definition of processes A−C; potentials referred to SCE.

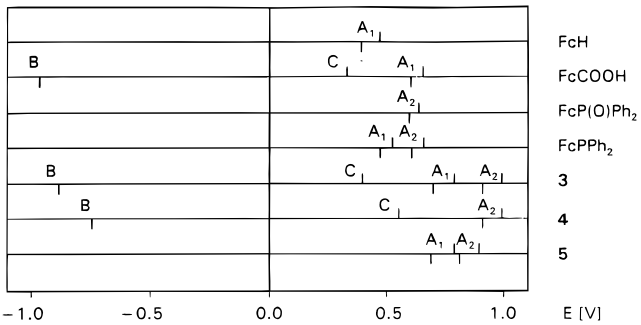

Figure 6. Trends in potentials of processes A−C.

Scheme 2

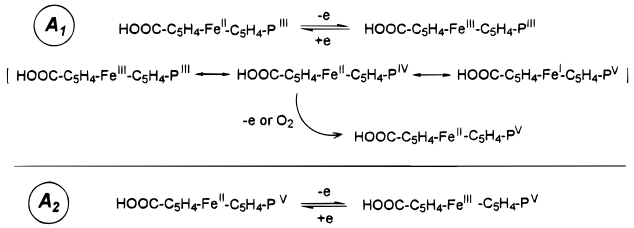

by the electron-withdrawing effect of the substituents. Diphenylphosphinyl and carboxyl group are strong electron acceptors which diminish the electron density at the ferrocene skeleton, thus making its oxidation more difficult. The lower value of the shift of the potential for $FcPPh_2$ is explainable by the weaker electron-accepting properties of the PPh_2 group (-I but +M substituent). For disubstituted ferrocenes **3**−**5**, the redox potentials of process A are shifted *vs* ferrocene by +310, +490, and +310 mV, respectively, thus pointing to the additivity of contributions of the substituents. The shifts are, however, by about 20% higher than the sum of the voltammetrically determined contributions of the monosubstituted derivatives, which may be explained by the absence of the "electron-buffering" effect of the unsubstituted Cp ring. Nevertheless, the redox potentials of process A [from CV as $^1/_2(E_{pa} + E_{pc})$] display linear corelation with Hammett's σ_p constants[13] of the substituents.

For the compounds containing carboxyl two further processes were observed. Process B is, most likely, the irreversible reduction of the carboxylic group.

Process C is the reversible oxidation of the product generated by the process B. After the electrolysis at a negative potential (−1.2 V) the oxidation peak on CV gains in intensity but, simultaneously, the anodic peak of the process A_1 diminishes such as the sum $i_{pa}(C) + i_{pa}(A_1)$ is constant. It appears that the process C is the ferro/ferri redox system of the ferrocene derivative bearing the reduced carboxyl group. The difference between the reduction potential of the process B and the oxidation potential of the process C is nearly constant for all compounds having the carboxyl group [$E_{pa}(C) - E_{pc}(B)$ is 1.30 V for FcCOOH and 1.29 V for both **3** and **4**], and therefore, it is likely that analogous products are formed in this process. The only difference is in the absolute potential values which are shifted in accordance with the electronic effects of the substituents (Figure 6).

In summary, the electrochemical results reflect the well-known phenomenon that, in substituted ferrocenes, the changes of the electron density located at the substituents are easily mediated through the fully conjugated π-electron system of the ferrocene skeleton. Such coupling of the redox centers is of crucial importance in the recent field of supramolecular electrochemistry.[14,15]

Experimental Section

General Considerations. NMR spectra: ^1H (200.06 MHz), $^{31}P\{^1H\}$ (80.98 MHz) on a Varian Unity 200 instrument; 2D (^1H observed at 499.843 MHz) and APT (^{13}C observed at 125.697 MHz) experiments on a Varian Unity 500 instrument; the standards were internal TMS for ^1H, the solvent signal for ^{13}C ($C[^2H]Cl_3$, δ 77.0), and external 85% aqueous H_3PO_4 for ^{31}P. All spectra were recorded in $C[^2H]Cl_3$ at room temperature (2D experiments at a probe temperature of 30 °C). Mass spectra were measured on a JEOL D-100 instrument (EI, 80 eV). Exact *m/z* values were obtained by the peak-match method with perfluorokerosene as the internal standard. IR spectra were measured in Nujol mulls between KBr windows in the range of 400−4000 cm^{-1} on an FT IR ATI Mattson Genesis instrument. UV/vis spectra were recorded in DME solutions on a Specord M40 (Carl Zeiss, Jena, Germany) instrument. The mp's are uncorrected. Electrochemical measurements were carried out at room temperature in an argon atmosphere with (3−8) × 10^{-4} M acetonitrile solutions containig 0.05 M Bu_4NPF_6 as the supporting electrolyte. The standard three-electron system consisted of a stationary platinum disk electrode of 2 mm diameter, an auxiliary platinum wire electrode, and a saturated calomel electrode (to which all potentials are referenced) separated from the solution by a double salt bridge. In RDE measurements,

(13) Exner, O. *Correlations in Organic Chemistry* (in Czech); SNTL Alfa Publishers: Prague, 1981.

(14) Texeira, M. G.; Roffia, S.; Bignozzi, C. A.; Paradisi, C.; Paolucci, F. *J. Electroanal. Chem.* **1993**, *345*, 243.

(15) Medina, J. C.; Goodnow, T. T.; Rojas, M. T.; Atwood, J. T.; Lynn, B. C.; Kaifer, A. E.; Gokel, G. W. *J. Am. Chem. Soc.* **1992**, *114*, 10583.

the platinum disk electrode rotated at 500 rpm. A Multipurpose Polarograph GWP 673 (ZWG, Berlin, East Germany) linked to an X-Y recorder served for the registration of voltammograms as well as the potentiostat for electrolyses. The potential was scanned at 500 and 250 mV min^{-1} for RDE and CV measurements, respectively.

1′-(Diphenylphosphino)ferrocenecarboxylic Acid (3). In a dry argon atmosphere, phenyllithium (28 mL of 1.8 mol dm^{-3} solution in 70:30 v/v cyclohexane/diethyl ether, 50.4 mmol) was added with cooling (solid carbon dioxide/*i*-PrOH bath) to a stirred precooled solution of **1**[7,8] (7.5 g, 25.7 mmol) in diethyl ether (400 mL). After being stirred for 30 min with cooling and then for 40 min without cooling, the reaction mixture was cooled again, poured onto powdered solid carbon dioxide (110 g, excess), and allowed to stand overnight. The subsequent operations were carried out in air. The reaction mixture was extracted by 5% aqeous sodium hydroxide (250 mL in four portions), and the combined extracts were acidified toward Congo Red with ice-cold 6 M aqueous HCl. The precipitated crude product was washed with ice-cold 1% aqueous HCl and dissolved in chloroform (350 mL). The solution was dried with magnesium sulfate and evaporated to dryness at reduced pressure. After crystallization from 50% v/v aqueous acetic acid by slow cooling of hot concentrated solution to 0 °C, washing with petroleum ether presaturated with acetic acid and then with petroleum ether, and drying over sodium hydroxide, pure **3** (7.6 g, 71%) was obtained as orange plates, mp 164.5−166 °C. Anal. Calcd for $C_{23}H_{19}FeO_2P$: C, 66.69; H, 4.62. Found: C, 66.6; H, 4.5. IR in Nujol [cm^{-1} (relative intensity), assignment]: 497 (s), 823 (m), 1090 (m), Fc; 1025 (m), 1153 (s), Ph; 1666 (s), COOH. MS (direct inlet, 170−180 °C; *m/z*, relative intensity, elemental composition, MW calcd/found): 414 ($M^{+\bullet}$, 100%, $C_{23}H_{19}FeO_2P$, 414.0472/414.0484); 386 ($[M - CO]^{+\bullet}$, 7%, $C_{22}H_{19}FeOP$, 386.0523/386.0514); 370 ($[M - CO_2]^{+\bullet}$, 33%, $C_{22}H_{19}FeP$, 370.0574/370.0520); 321 (18%, $C_{17}H_{14}FeOP$, 321.0132/321.0102); 293 (28%, $C_{16}H_{14}FeP$, 293.0182/293.0174). UV/vis [λ_{max} (nm), ϵ (m^2 mol^{-1})]: 443 (23).

1′-(Diphenylphosphinoyl)ferrocenecarboxylic Acid (4). A solution of 30% aqueous hydrogen peroxide (2 mL, excess) was added to a stirred solution of **3** (0.20 g, 0.48 mmol) in acetone (15 mL). After 1 h at room temperature, a further 1 mL of the H_2O_2 solution was added and the mixture was refluxed for 90 min. The solution was evaporated at reduced pressure, the product was extracted into chloroform, and the extract was evaporated and crystallized as for **3** to give **4** (90 mg, 43%) as rusty red prismatic crystals, dec 195 °C without melting. Anal. Calcd for $C_{23}H_{19}FeO_3P$: C, 64.21; H, 4.45. Found: C, 64.1; H, 4.5. IR (as above): 491 (m), 834 (s), 1099 (m), Fc; 1025 (s), 1150 (m), Ph; 1110−1200 (s), P═O; 1696−1703 (s), COOH. MS not measured (decomposition on attempted direct inlet). UV/vis (as above): 442 (saturated solution).

Methyl 1′-(Diphenylphosphino)ferrocenecarboxylate (5). A solution of diazomethane in diethyl ether (approximately 2-fold excess) was added to a solution of **3** (0.41 g, 0.99 mmol) in diethyl ether (20 mL), and the mixture was stirred at room temperature for 30 min and then refluxed for further 30 min. After evaporation at reduced pressure, the crude product was dissolved in boiling methanol (30 mL) and crystallized on addition of water (30 mL) to the hot solution and slow cooling. The product was washed with petroleum ether presaturated with methanol and then with petroleum ether and dried in air to give **5** (0.30 g, 71%) as orange flakes, mp 118.5−119.5 °C. Anal. Calcd for $C_{24}H_{21}FeO_2P$: C, 67.31; H, 4.94. Found: C, 67.4; H, 4.9. IR (as above): 490 (m), 830 (s), 1090 (m), Fc; 1026 (m), 1145 (s), Ph; 1710 (s), C═O. MS (direct inlet at 120 °C): 428 ($M^{+\bullet}$, 100%, $C_{24}H_{21}FeO_2P$, 428.0628/428.0638); 413 ($[M - CH_3]^+$, 25%, $C_{23}H_{18}FeO_2P$, 413.0394/413.0383); 397 ($[M - OCH_3]^+$, 2%); 351 ($[M - C_6H_5]^+$, 7%, $C_{18}H_{16}FeO_2P$, 351.0237/351.0232); 321 (50%, $C_{17}H_{14}FeOP$, 321.0132/321.0131). UV/vis: 445 (25).

Table 5. Crystallographic Data for 3−5

	3	**4**	**5**
(a) Crystal Parameters			
formula	$C_{23}H_{19}FeO_2P$	$C_{23}H_{19}FeO_3P$	$C_{24}H_{21}FeO_2P$
MW	414.05	430.05	428.06
cryst system	triclinic	monoclinic	monoclinic
space group	$P\bar{1}$ (No. 2)	$P2_1/c$ (No. 14)	$P2_1/c$ (No. 14)
a, Å	5.9189(6)	12.738(1)	8.4113(8)
b, Å	13.814(1)	12.4813(8)	17.2130(2)
c, Å	23.234(2)	12.388(1)	14.1817(9)
α, deg	86.852(6)		
β, deg	82.980(8)	96.994(8)	95.360(6)
γ, deg	77.640(7)		
V, Å	1920.3(3)	1954.8(3)	2044.3(2)
Z	4	4	4
d(calcd), g/cm^3	1.433	1.462	1.391
d(measd), g/cm^3 [a]	1.43	1.45	
μ(Mo, Kα), mm^{-1}	0.884	0.875	0.832
temp, K	296(2)	296(2)	296(2)
cryst size, mm	0.07 × 0.18 × 0.29	0.08 × 0.21 × 0.25	0.20 × 0.32 × 0.70
color	orange	rusty red	orange
(b) Data Collection			
scan limits (*θ*), deg	0−25	0−24	0−25
data collcd			
h	−6, 7	−14, 14	−9, 9
k	−16, 16	−14, 0	0, 20
l	0, 28	−14, 14	0, 16
reflcns collcd	6720	6119	3864
reflcns unique	6720	3059	3582
reflcns obsd ($F_o \geq 4\sigma(F_o)$)	3725	2021	2762
std reflcns		3 after every 1 h	
var in stds, %	4	2	2
(c) Refinement			
R(*F*), %[b]	4.07	3.06	3.24
R(wF), %[c]	7.92	6.59	7.99
GOF[d]	1.110	1.050	1.038
Δ/*σ*(max)	0.001	0.001	−0.001
Δ(*ρ*), e/Å^3	±0.28	−0.22; 0.24	−0.43; 0.23
N_o/N_v	6701/495	3059/257	3582/262

[a] Flotation in aqueous $ZnBr_2$. [b] $R(F) = \sum(||F_o| - |F_c||)/\sum|F_o|$ for observed reflections. [c] $R(wF) = \sum(w^{1/2}(|F_o| - |F_c|)/w^{1/2}|F_o|)$; $w = [\sigma^2(F_o^2) + w_1P^2 + w_2P]^{-1}$; $P = [max(F_o^2) + 2F_c^2]/3$; w_1 (w_2) = 0.0337 (0.87) for **3**, 0.0364 (0.10) for **4**, and 0.0453 (0.60) for **5**. [d] GOF = $(\sum(w||F_o| - |F_c||)/(N_o - N_v))^{1/2}$.

X-ray Structure Determinations of 3−5. An orange, platelike crystal of **3** was grown from 50% aqueous acetic acid by slow cooling. A rusty red prismatic crystal of **4** was selected from the preparative batch. An orange prismatic crystal of **5** was grown from methanol presaturated with heptane by slow evaporation. The crystals were mounted on glass fibers with epoxy cement. All measurements were carried out on an Enraf Nonius CAD4 diffractometer at 23 °C using graphite-monochromated Mo Kα radiation (λ = 0.710 73 Å). Data were collected by $\omega-2\theta$ scans. Absorption was neglected. Further crystallographic details are sum-

Table 6. Fractional Atomic Coordinates ($\times 10^4$) and Equivalent Isotropic Displacement Parameters[a] (Å^2 $\times$ 10^3) for 3

	x	*y*	*z*	*U*(eq)		*x*	*y*	*z*	*U*(eq)
Fe(1)	368(1)	1841(1)	1046(1)	39(1)	P(2)	962(2)	4906(1)	2989(1)	42(1)
P(1)	−1142(2)	93(1)	2011(1)	43(1)	O(21)	2788(6)	712(3)	4742(1)	55(1)
O(11)	−1751(6)	4285(3)	258(1)	53(1)	O(22)	5858(6)	1202(3)	5007(1)	56(1)
O(12)	2060(6)	3803(3)	−8(1)	56(1)	C(201)	3119(7)	3834(3)	3181(2)	36(1)
C(101)	145(7)	1164(3)	1817(2)	38(1)	C(202)	2853(8)	2837(3)	3160(2)	43(1)
C(102)	−1141(8)	2161(3)	1838(2)	43(1)	C(203)	4849(9)	2200(4)	3337(2)	52(1)
C(103)	393(9)	2794(4)	1666(2)	51(1)	C(204)	6368(8)	2786(4)	3467(2)	52(1)
C(104)	2628(9)	2214(4)	1536(2)	52(1)	C(205)	5332(8)	3792(4)	3373(2)	44(1)
C(105)	2498(8)	1208(4)	1627(2)	45(1)	C(206)	2858(8)	2413(3)	4700(2)	40(1)
C(106)	−31(8)	2590(3)	305(2)	40(1)	C(207)	3854(8)	3242(4)	4763(2)	46(1)
C(107)	−2083(9)	2227(4)	502(2)	48(1)	C(208)	2293(10)	4102(4)	4605(2)	57(1)
C(108)	−1431(9)	1191(4)	556(2)	54(1)	C(209)	314(9)	3812(4)	4446(2)	55(1)
C(109)	978(10)	892(4)	399(2)	58(1)	C(210)	649(8)	2776(4)	4498(2)	47(1)
C(110)	1861(9)	1759(4)	237(2)	49(1)	C(211)	3826(8)	1368(4)	4812(2)	43(1)
C(111)	15(9)	3629(4)	191(2)	43(1)	C(212)	1996(8)	5914(3)	3273(2)	47(1)
C(112)	1201(8)	−917(3)	1725(2)	43(1)	C(213)	857(9)	6319(4)	3766(2)	62(2)
C(113)	919(11)	−1311(4)	1233(2)	62(2)	C(214)	1602(13)	7040(4)	4016(2)	83(2)
C(114)	2659(13)	−2036(5)	983(2)	82(2)	C(215)	3492(13)	7381(5)	3778(3)	83(2)
C(115)	4653(12)	−2386(5)	1216(3)	82(2)	C(216)	4661(11)	7010(4)	3286(3)	80(2)
C(116)	4954(10)	−2014(5)	1711(3)	79(2)	C(217)	3906(10)	6288(4)	3036(2)	63(2)
C(117)	3213(9)	−1284(4)	1960(2)	65(2)	C(218)	1906(8)	5018(3)	2244(2)	40(1)
C(118)	−821(7)	−19(3)	2758(2)	39(1)	C(219)	4096(8)	4593(4)	1997(2)	49(1)
C(119)	690(8)	413(4)	3005(2)	50(1)	C(220)	4699(9)	4675(4)	1426(2)	58(1)
C(120)	786(9)	311(4)	3576(2)	60(1)	C(221)	3097(11)	5206(4)	1108(2)	67(2)
C(121)	−598(10)	−214(4)	3897(2)	68(2)	C(222)	931(11)	5626(5)	1338(2)	76(2)
C(122)	−2114(10)	−626(5)	3660(2)	77(2)	C(223)	336(9)	5534(4)	1903(2)	58(1)
C(123)	−2225(9)	−538(4)	3096(2)	58(1)	H(91)	1918(99)	4537(54)	−92(26)	113(23)
Fe(2)	3256(1)	3158(1)	3954(1)	39(1)	H(92)	6215(68)	592(33)	5101(17)	33(13)

[a] *U*(eq) is defined as one-third of the trace of the orthogonalized $\mathbf{U}_{ij}$ tensor.

Table 7. Fractional Atomic Coordinates ($\times 10^4$) and Equivalent Isotropic Displacement Parameters[a] (Å^2 $\times$ 10^3) for 4

	x	*y*	*z*	*U*(eq)
Fe	9035(1)	2672(1)	8687(1)	37(1)
P	6775(1)	1343(1)	7882(1)	38(1)
O(1)	12254(2)	3495(2)	7131(2)	60(1)
O(2)	11559(2)	4273(2)	8758(2)	64(1)
O(3)	7275(2)	642(2)	7119(2)	51(1)
C(01)	7465(2)	2578(2)	8164(2)	37(1)
C(02)	8008(2)	3138(3)	7395(3)	44(1)
C(03)	8486(2)	4044(3)	7918(3)	53(1)
C(04)	8262(3)	4062(3)	8991(3)	56(1)
C(05)	7630(2)	3159(3)	9160(3)	47(1)
C(06)	10615(2)	2668(3)	8627(2)	39(1)
C(07)	10142(2)	1753(2)	8077(3)	46(1)
C(08)	9657(2)	1150(3)	8835(3)	52(1)
C(09)	9820(2)	1675(3)	9841(3)	57(1)
C(10)	10406(2)	2614(3)	9722(2)	49(1)
C(11)	11169(2)	3514(2)	8086(3)	41(1)
C(12)	6668(2)	731(2)	9175(2)	38(1)
C(13)	7290(2)	−163(2)	9473(2)	45(1)
C(14)	7237(3)	−642(3)	10470(3)	55(1)
C(15)	6584(3)	−247(3)	11167(3)	55(1)
C(16)	5967(3)	625(3)	10880(3)	56(1)
C(17)	6010(2)	1120(3)	9897(3)	47(1)
C(18)	5448(2)	1688(2)	7300(3)	45(1)
C(19)	4967(3)	1063(3)	6455(3)	63(1)
C(20)	3935(3)	1295(4)	6000(3)	82(1)
C(21)	3399(3)	2132(4)	6398(4)	86(2)
C(22)	3867(3)	2741(3)	7227(4)	75(1)
C(23)	4887(2)	2536(3)	7676(3)	58(1)
H(99)	11835(27)	4706(27)	8451(27)	48(11)

[a] *U*(eq) is defined as one-third of the trace of the orthogonalized $\mathbf{U}_{ij}$ tensor.

Table 8. Fractional Atomic Coordinates ($\times 10^4$) and Equivalent Isotropic Displacement Parameters[a] (Å^2 $\times$ 10^3) for 5

	x	*y*	*z*	*U*(eq)
Fe	7101(1)	3260(1)	8527(1)	49(1)
P	3785(1)	2094(1)	8342(1)	43(1)
O(1)	10636(2)	4658(2)	8911(1)	80(1)
O(2)	8421(2)	5259(1)	8296(1)	72(1)
C(01)	5199(3)	2708(1)	9029(2)	45(1)
C(02)	5043(4)	3532(2)	9097(2)	63(1)
C(03)	6375(5)	3816(2)	9676(2)	82(1)
C(04)	7349(4)	3190(2)	9968(2)	81(1)
C(05)	6649(3)	2505(2)	9576(2)	57(1)
C(06)	8683(6)	3956(2)	7944(2)	52(1)
C(07)	7236(3)	3913(2)	7340(2)	55(1)
C(08)	7003(4)	3125(2)	7090(2)	70(1)
C(09)	8259(4)	2688(2)	7528(2)	79(1)
C(10)	9308(4)	3191(2)	8057(2)	70(1)
C(11)	9373(3)	4643(2)	8436(2)	57(1)
C(12)	4981(3)	1216(1)	8206(2)	41(1)
C(13)	5495(3)	1067(1)	7322(2)	51(1)
C(14)	6460(3)	433(2)	7180(2)	61(1)
C(15)	6893(3)	−65(2)	7911(2)	59(1)
C(16)	6371(3)	65(1)	8785(2)	54(1)
C(17)	5425(3)	700(1)	8934(2)	48(1)
C(18)	2500(2)	1785(1)	9253(2)	41(1)
C(19)	2557(3)	2098(2)	10150(2)	53(1)
C(20)	1462(3)	1880(2)	10775(2)	62(1)
C(21)	311(3)	1343(2)	10508(2)	65(1)
C(22)	239(3)	1020(2)	9621(2)	66(1)
C(23)	1325(3)	1237(2)	8994(2)	56(1)
C(24)	8924(7)	5964(2)	8783(3)	102(2)
H(24A)	9073(48)	5914(23)	9439(30)	123
H(24B)	8256(51)	6345(26)	8597(29)	123
H(24C)	10088(49)	6141(25)	8600(27)	123

[a] *U*(eq) is defined as one-third of the trace of the orthogonalized $\mathbf{U}_{ij}$ tensor.

marized in Table 5. The structures were solved by combination of heavy atom and direct methods (SHELXS-86[16]) and refined by a full-matrix least-squares procedure based on F^2 (SHELXL93[17]). Hydrogen atoms of cyclopentadienyl and phenyl groups were fixed in calculated positions [C−H = 0.96 Å, $U_{iso}(H) = 1.2U_{iso}(C)$]; those of carboxyl and methyl groups found from the difference maps were refined isotropically. The final

(16) Sheldrick, G. M. *Acta Crystallogr.* **1990**, *A46*, 467.

(17) Sheldrick, G. M. SHELXL93: A computer program for crystal structure refinement; University of Göttingen, Germany, 1993.

difference Fourier map had no peaks of chemical significance. Scattering factors were those implemented in the SHELX programs. Positional parameters are given in Tables 6−8.

Acknowledgment. Financial support for this work was given by the Grant Agency of the Czech Republic through Grant Nos. 203/93/0244, 203/93/2463, and 203/93/0154.

Supporting Information Available: Crystallographic data for **3**−**5**, including tables of H coordinates and thermal parameters, anisotropic thermal parameters of non-H atoms, complete bond distances and angles, and least-squares planes and atomic deviations therefrom and unit cell diagrams, Cambridge Crystallographic Database search tables including GSTAT query and statistics, and text providing detailed discussion of NMR spectra (22 pages). Ordering information is given on any current masthead page.

OM950528Q